AJNR

Septum orbitale: high-resolution MR in orbital anatomy.

K T Hoffmann, N Hosten, A J Lemke, B Sander, C Zwicker and R Felix

AJNR Am J Neuroradiol 1998, 19 (1) 91-94
http://www.ajnr.org/content/19/1/91

AJNR Am J Neuroradiol 19:91–94, January 1998

Septum Orbitale: High-Resolution MR in Orbital Anatomy

K-T. Hoffmann, N. Hosten, A-J. Lemke, B. Sander, C. Zwicker, and R. Felix

PURPOSE: **The purpose of this study was to ascertain whether MR imaging, with the use of a surface coil, can accurately show small intraorbital structures; in particular, the septum orbitale.**

METHODS: **Examinations of 26 patients who underwent unilateral orbital high-resolution MR imaging for different indications were evaluated to differentiate the septum orbitale from related structures, such as the aponeurosis of the levator palpebrae, the superior tarsal (Müller's) muscle, and the superior orbital (Whitnall's) ligament.**

RESULTS: **A subtle differentiation of the septum orbitale was obtained in 23 patients (88%) and of the levator aponeurosis and Müller's muscle in 24 patients (92%). The orbicularis oculi muscle and the submuscular fibroadipose tissue were reliably identified in all patients.**

CONCLUSIONS: **High-resolution MR imaging is suitable for differentiating small intraorbital structures. Nevertheless, an exact depiction of the septum orbitale remains very much dependent on the cooperation of the patient. The site of orbital disease can be determined precisely and in a noninvasive manner in relation to the septum orbitale.**

The septum orbitale is one part of the palpebral anatomic system, which also includes the skin with the subcutaneous tissue, the palpebral part of the orbicularis oculi muscle and the submuscular fibroadipose layer, the tarsi, the preaponeurotic fat, the eyelid retractors, and the conjunctiva (1). It is thought to be derived from mesenchyme of the second embryonic arch (2). The septum orbitale constitutes the anterior border of the orbit by separating intraorbital fat from eyelid fat and from the orbicularis oculi muscle. The septum maintains intraorbital fat in its position. It is presumed that dehiscence of the septum and fibers in the preseptal fibroadipose layer are essential for the herniation of intraorbital fat into palpebral compartments, causing fatty pseudopouches and, eventually, bulging eyelids in the course of aging (3). Besides this function, the septum orbitale is involved in ocular and palpebral movements. It is attached to the orbital arcus marginalis and fuses with the levator aponeurosis 2 to 5 mm above the superior border of the tarsus in the Occidental upper lid and with the inferior border of the tarsus in the lower lid (4). In the Asian upper lid, the septum orbitale fuses with the aponeurosis of the levator palpebrae below the superior tarsal border, causing the distinctive appearance of Asian eyelids (5).

Dissection and surgery have provided detailed information on eyelid anatomy. Steady improvements in magnetic resonance (MR) imaging techniques, such as phased-array and small surface coils as well as optimized pulse sequences (currently reaching submillimeter resolution), have contributed to noninvasive anatomic research as well as to recent advances in diagnostic procedures (6–8). We report our findings in a study of orbital structures, conducted to determine the accuracy of high-resolution MR imaging in delineating the septum orbitale and related structures, and in defining their spatial relation to orbit or eyelid-associated abnormalities, respectively.

Methods

We retrospectively reviewed the imaging studies of 26 patients, of whom 13 were examined for extraocular orbital disease (lymphoma [n = 3], squamous cell carcinoma of the upper [n = 1] or lower [n = 2] eyelid, suspected lymphangioma [n = 2], metastases [n = 3], dermoid cyst [n = 1], epidermoid [n = 1]) and 13 for intraocular disease (choroidal melanoma [n = 12], retinoblastoma [n = 1]). Unilateral orbital MR imaging was performed on a 1.5-T superconductive system (Magnetom SP 63, Siemens AG, Germany) using a receive-only radio-frequency surface coil with a diameter of 4 cm. In each patient, both T1-weighted (600/20/2 [repetition time/echo time/excitations]); field of view, 60 mm; matrix, 256 × 256 pixels; section thickness, 2 mm without gap) and T2-weighted (2300–4600/90/1; field of view, 130 mm; matrix, 240 × 256 pixels; section thickness, 2 mm without gap) spin-echo sequences were acquired. T1-weighted sequences were obtained

Received December 18, 1996; accepted after revision July 14, 1997.

From the Strahlenklinik und Poliklinik, Virchow Klinikum der Humboldt Universität zu Berlin (Germany).

Address reprint requests to K-T. Hoffmann, MD, Strahlenklinik und Poliklinik, Klinikum Rudolf Virchow, Augustenburger Platz 1, 13353 Berlin, Germany.

in sagittal, axial, or coronal planes, providing an in-plane resolution of approximately 0.23 mm. T2-weighted spin-echo or turbo spin-echo sequences were obtained in an axial plane. Only T1-weighted images were considered for evaluation owing to their superior spatial resolution and contrast between fat and musculoligamentary structures. All imaging studies were evaluated by two radiologists for delineation of the septum orbitale and related structures, such as the levator aponeurosis, the levator tarsi muscle, the orbicularis oculi muscle, and the submuscular fibroadipose layer. The spatial relationship between orbital or palpebral disease and the septum orbitale was determined.

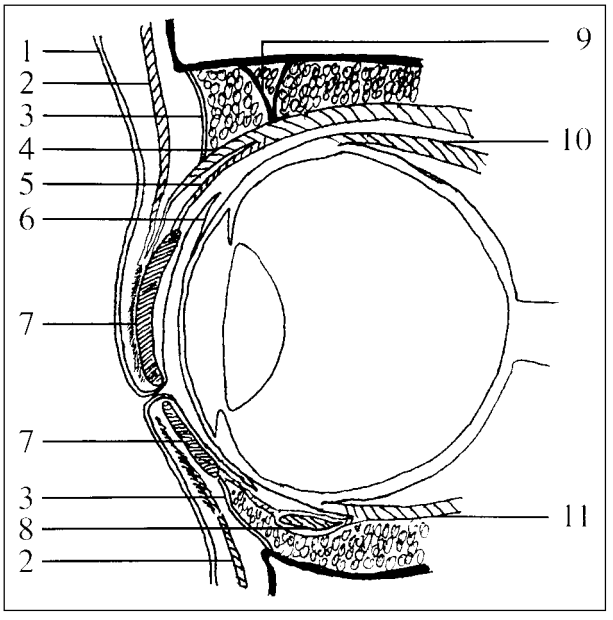

FIG 1. Schematic cross section of anterior orbital and palpebral anatomy. *1* indicates skin; *2*, orbicularis oculi muscle; *3*, septum orbitale; *4*, levator aponeurosis; *5*, levator tarsi superior (Müller's) muscle; *6*, conjunctiva; *7*, tarsus; *8*, inferior oblique muscle; *9*, superior orbital (Whitnall's) ligament; *10*, superior rectus muscle; and *11*, inferior rectus muscle.

Results

Figure 1 is a schematic drawing of the structures of interest. High-resolution MR images of the orbit are presented in Figures 2 through 5. In 23 (88%) of the imaging studies, the septum orbitale was clearly identified as descending from the superior orbital rim and fusing with the levator aponeurosis before reaching the superior edge of the tarsus in the upper lid and ascending from the inferior orbital rim toward the tarsus in the lower lid. The distance between the superior border of the upper tarsus and fusion of the septum with the levator aponeurosis exceeded 5 mm in more than half (n = 19) the cases reviewed. These results differ from previously described anatomic findings (1, 4) and may be explained by the limited spatial resolution of MR imaging, in that closely adjoining structures are depicted as one. Differentiation of the septum was more difficult to obtain in the lower lid than in the upper lid. In particular, in older patients, intraorbital fat generally caused the inferior septum to curve toward the orbicularis oculi muscle, contributing to the appearance of a bulging eyelid (Fig 2).

According to anatomic findings described by Doxanas et al (5), the appearance of the septum changes between that of a singular sheet and that of more or less closely adjoining thin layers. Especially in the latter view, it may be difficult to obtain a clear distinction of the superior orbital (Whitnall's) ligament, since it cannot be reliably identified in the interposed preaponeurotic fat. Whitnall's ligament descends from the orbital roof and is attached to the levator aponeurosis muscle. It is considered a suspender (ad-

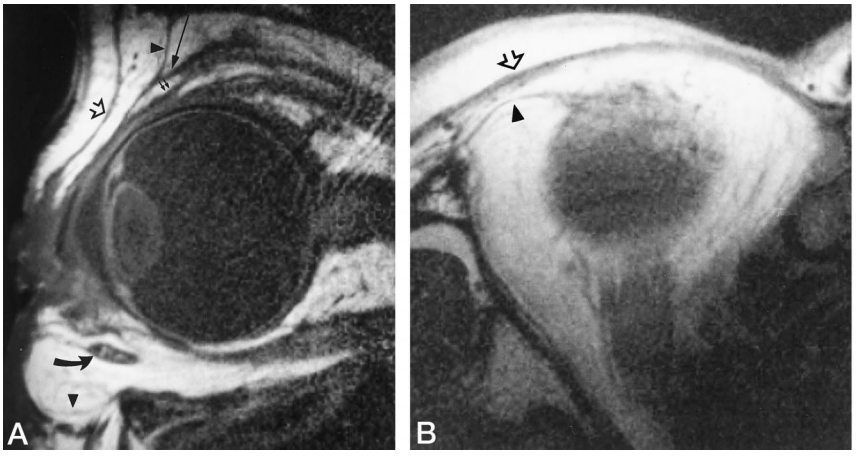

FIG 2. *A*, T1-weighted sagittal MR image (600/20/2) of the left orbit of a 69-year-old patient with malignant corpus ciliare melanoma (not shown). Note the bulging lower lid due to the pressure of the intraorbital fat. *Arrowheads* indicate septum orbitale; *open arrow,* orbicularis oculi muscle; *long arrow,* levator aponeurosis; *small arrows,* levator tarsi superior (Müller's) muscle; and *curved arrow,* inferior oblique muscle.

B, Axial T1-weighted image (600/20/2) of the lower lid in the same patient. The temporal part of the slightly bulging septum orbitale (*arrowhead*) is depicted behind the palpebral part of the orbicularis oculi muscle (*arrow*). The interposed fibroadipose layer has high signal intensity.

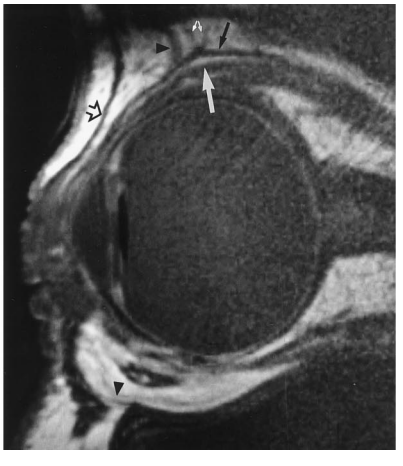

FIG 3. T1-weighted sagittal MR image (600/20/2) of the left orbit of a 56-year-old patient with malignant choroidal melanoma (not shown) and artificial lens. The V-shaped Whitnall's ligament (*small white arrows*) between orbital roof and levator palpebrae muscle (*solid black arrow*, levator aponeurosis; *large white arrow*, Müller's muscle) is clearly depicted. *Arrowheads* indicate orbitale; *open arrow*, orbicularis oculi muscle.

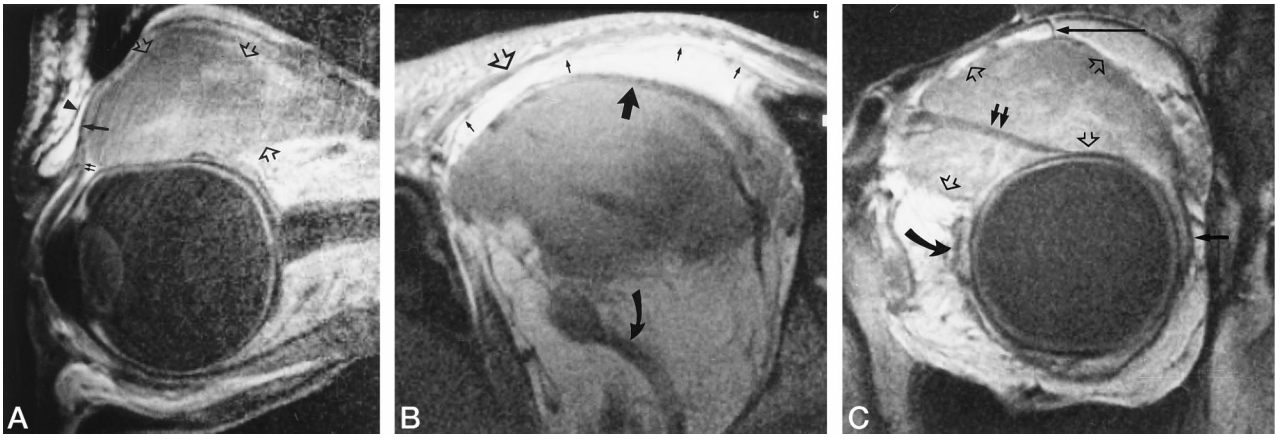

FIG 4. *A*, T1-weighted sagittal MR image (600/20/2) of the right orbit of a 52-year-old patient with orbital manifestation of a malignant lymphoma (*open arrows*). The globe is impressed by the extended mass, and differentiation of the superior rectus muscle is not possible. The levator palpebrae muscle (*single solid arrow,* levator aponeurosis; *double arrows,* levator tarsi superior [Müller's] muscle) and the septum orbitale (*arrowhead*) are displaced.

B, T1-weighted axial image (600/20/2) of the same patient allows almost continuous differentiation of the septum (*small arrows*), which is "embedded" in the hyperintense fibroadipose layer behind the orbicularis oculi muscle (*open arrow*) and the preaponeurotic fat in front of the levator palpebrae (*large straight arrow*). The tumor with medium signal intensity is limited anteriorly by the levator palpebrae muscle. *Curved arrow* indicates ophthalmic vein.

C, Coronal T1-weighted image (600/20/2) does not contribute to improved delineation of the septum orbitale, most probably because of its orientation. The tumor extent (*open arrows*) is seen in relation to the globe circumference, with insertions of the lateral (*single straight arrow*) and medial (*curved arrow*) rectus muscle, as well as to the superior oblique muscle (*double arrows*) and the orbital roof, with a section of Whitnall's ligament depicted (*long arrow*).

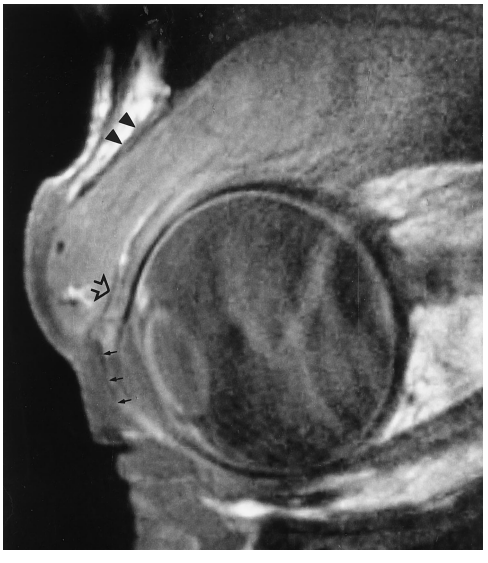

FIG 5. T1-weighted sagittal MR image (600/20/2) of the left orbit of a 48-year-old patient with non-Hodgkin lymphoma. The large intraorbital mass, occupying the postseptal space, curves the palpebral part of the orbicularis oculi muscle as well as the tarsus (*small arrows*) and stretches the septum orbitale (*arrowheads*). The thickened appearance of the septum is probably due to closely adjoining fibers of the levator aponeurosis. *Open arrow* indicates levator tarsi superior muscle.

ditional to the radial connective tissue septa of the superior orbit) while simultaneously applying a vector-changing force to the levator aponeurosis (8, 9). The V-shaped appearance of Whitnall's ligament is shown in Figure 3. In two cases of orbital lymphoma, the dislocation of the septum orbitale by postseptal masses did not reduce its detectability on sagittal and axial images (Fig 4). In another patient, with intraorbital manifestation of non-Hodgkin lymphoma involving the superior rectus and the levator palpebrae muscles, clear differentiation of the extended septum from closely adjoining fibers of the dislocated levator aponeurosis was not obtained (Fig 5). This case emphasizes the role of the septum as a sufficiently working border between the intraorbital and the extraorbital compartments. Preaponeurotic fat was generally identified posterior to the septum orbitale and anterior to the levator aponeurosis in the upper lid, and anterior to the inferior retractors in the lower lid, respectively. A subtle distinction between the levator aponeurosis and Müller's muscle was obtained in 24 imaging studies (92%). The palpebral part of the orbicularis oculi muscle and the posteriorly adjoining submuscular fibroadipose layer, with variable accentuation of its lobulated structure and fibrous septa, were clearly identified on all imaging studies.

Discussion

High-resolution MR images provide an excellent depiction of even minute intraorbital structures. This subtle delineation of the palpebral layers, the septum orbitale, and the levator muscles makes MR imaging superior to other techniques. Distinguishing between the preseptal and postseptal space is of value in defining and classifying orbital disease and for preoperative anatomic staging. In infectious diseases of the orbit, proper identification of the site of infection may lead to different therapeutic approaches, depending on involvement of the preseptal or postseptal intraorbital space (10). With regard to tumors of the anterior

orbit and eyelid, MR imaging can provide surgeons with additional information regarding the septum orbitale and its integrity. In eyelid-related surgery for blepharoplasty, except for the transconjunctival approach, an adequate imaging study may help the surgeon determine more precisely the site of the septum orbitale in the evacuation of intraorbital fat (11). High-resolution MR imaging can, therefore, be useful in helping to precisely determine the site of orbital abnormality in relation to the septum orbitale.

References

1. Dailey RA, Wobig JL. **Eyelid anatomy**. *J Dermatol Surg Oncol* 1992;18:1023–1027
2. Gasser RF. **The development of facial muscles in man**. *Am J Anat* 1966;120:357–376
3. Brémond-Gignac DS, Deplus S, Cussenot O, Lassau JP. **Anatomic study of the orbital septum**. *Surg Radiol Anat* 1994;16:121–124
4. Meyer DR, Linberg JV, Wobig JL, McCormick SA. **Anatomy of the orbital septum and associated eyelid connective tissues**. *Ophthal Plast Reconstr Surg* 1991;7:104–113
5. Doxanas MT, Anderson RL. **Oriental eyelids**. *Arch Ophthalmol* 1984;102:1232–1235
6. Breslau J, Dalley RW, Tsuruda JS, Hayes CE, Maravilla KR. **Phased-array surface coil MR of the orbits and optic nerves**. *AJNR Am J Neuroradiol* 1995;16:1247–1251
7. Hosten N, Lemke AJ, Sander B, et al. **MR anatomy and small lesions of the eye: improved delineation with a special surface coil**. *Eur Radiol* 1997;7:459–463
8. Ettl A, Priglinger S, Kramer J, Koornneef L. **Functional anatomy of the levator palpebrae superioris muscle and its connective tissue system**. *Br J Ophthalmol* 1996;80:702–707
9. Goldberg RA, Wu JC, Jesmanowicz A, Hyde JS. **Eyelid anatomy revisited**. *Arch Ophthalmol* 1992;110:1598–1600
10. Piazza P, Comoretto M, Lutmann M. **Computed tomography in acute inflammation of the orbit**. *Radiol Med Torino* 1994;87:235–239
11. Yousif NJ, Sonderman P, Dzwierzynski WW, Larson DL. **Anatomic considerations in transconjunctival blepharoplasty**. *Plast Reconstr Surg* 1995;96:1271–1278